

# FORMATION OF SEASONAL ICE BODIES AND ASSOCIATED CRYOGENIC CARBONATES IN CAVERNE DE L'OURS, QUÉBEC, CANADA: KINETIC ISOTOPE EFFECTS AND PSEUDO-BIOGENIC CRYSTAL STRUCTURES

DENIS LACELLE<sup>1</sup>, BERNARD LAURIOL<sup>2</sup>, AND IAN D. CLARK<sup>3</sup>

**Abstract:** This study examines the kinetics of formation of seasonal cave ice formations (stalagmites, stalactites, hoar, curtain, and floor ice) and the associated cryogenic calcite powders in Caverne de l'Ours (QC, Canada), a shallow, thermally-responsive cave. The seasonal ice formations, which either formed by the: (1) freezing of dripping water (ice stalagmite and stalactite); (2) freezing of stagnant or slow moving water (floor ice and curtain ice) and; (3) condensation of water vapor (hoar ice), all (except floor ice) showed kinetic isotope effects associated with the rapid freezing of calcium – bicarbonate water. This was made evident in the  $\delta D$ ,  $\delta^{18}O$  and  $d$  (deuterium excess) compositions of the formed ice where they plot along a kinetic freezing line. The cryogenic calcite powders, which are found on the surface of the seasonal ice formations, also show kinetic isotope effects. Their  $\delta^{13}C$  and  $\delta^{18}O$  values are among the highest measured in cold-climate carbonates and are caused by the rapid rate of freezing, which results in strong C-O disequilibrium between the water, dissolved C species in the water, and precipitating calcite. Although the cryogenic calcite precipitated as powders, diverse crystal habits were observed under scanning electron microscope, which included rhombs, aggregated rhombs, spheres, needles, and aggregated structures. The rhomb crystal habits were observed in samples stored and observed at room temperature, whereas the sphere and needle structures were observed in the samples kept and observed under cryogenic conditions. Considering that the formation of cryogenic calcite is purely abiotic (freezing of calcium – bicarbonate water), the presence of spherical structures, commonly associated with biotic processes, might represent vaterite, a polymorph of calcite stable only at low temperatures. It is therefore suggested that care should be taken before suggesting biological origin to calcite precipitates based solely on crystal habits because they might represent pseudo-biogenic structures formed through abiotic processes.

## INTRODUCTION

Most terrestrial freshwaters have a chemistry dominated by  $Ca^{2+}$  and  $HCO_3^-$  solutes that originates from the preferential dissolution of calcareous components of the bedrock. Even in crystalline bedrock environments, where the bedrock can comprise less than 1% carbonate, calcite dissolution will dominate over silicate weathering due to the higher solubility of calcite over silicate (White et al., 1999). Therefore, when a solution containing both  $Ca^{2+}$  and  $HCO_3^-$  solutes freezes, precipitation of cryogenic calcite ( $CaCO_3$ ), or other forms of low-temperature carbonates, like vaterite ( $\mu$ - $CaCO_3$ ) and ikaite ( $CaCO_3 \cdot 6H_2O$ ), is expected, irrespective of the local geology. In the natural environment, cryogenic carbonates are quite common in areas where the air temperatures fall below the freezing point for at least a few months of the year. Freezing caves, located in areas of limestone bedrock, are among the most susceptible environments in which to find cryogenic carbonate precipitates (Clark and Lauriol, 1992; Zak et al., 2004; Lacelle, 2007; Zak et al., 2008; Richter and

Riechelmann, 2008). However, cryogenic carbonates are also commonly encountered on the surface of aufeis or river icings (Hall, 1980; Pollard, 1983; Clark and Lauriol, 1997; Lacelle et al., 2006) and on the surface of clasts (Hallet, 1976; Fairchild et al., 1993; Marlin et al., 1993; Courty et al., 1994). The most commonly precipitated carbonate mineral is calcite, but vaterite and ikaite have also been reported from some high Arctic and Antarctic environments (Pauly, 1963; Suess et al., 1982; Marion, 2001; Omelon et al., 2001; Grasby, 2003). However, these metastable minerals have never been identified in freezing caves.

Experimental work done by Hallet (1976), Fairchild et al. (1996), and Killawee et al. (1998) have shown that the formation of cryogenic carbonate minerals involved a

<sup>1</sup> Planetary Exploration and Space Astronomy, Canadian Space Agency, 6767 route de l'aéroport, St-Hubert, QC, J3Y 8Y9, Canada. denis.lacelle@asc-csa.gc.ca

<sup>2</sup> Department of Geography, University of Ottawa, 60 University St., Ottawa, ON, K1N 6N5, Canada. blauriol@uottawa.ca

<sup>3</sup> Department of Earth Sciences, University of Ottawa, 140 Louis Pasteur, Ottawa, ON, K1N 6N5, Canada. idclark@uottawa.ca

series of chemical processes and unique kinetics of dissolution leading to the precipitation of carbonates. During initial freezing of a calcium bicarbonate solution, the  $\text{Ca}^{2+}$  and  $\text{HCO}_3^-$  solutes increase to a point where eventually their ion activity product might reach and exceed the calcite saturation point, causing calcite to precipitate from the solution. During their experimental work, Fairchild et al. (1996) identified the precipitation of both calcite and vaterite minerals, represented by rhombs (or aggregated rhombs) and spheres, respectively. For cryogenic calcite precipitated under equilibrium conditions, it was recently demonstrated by Lacelle et al. (2006) that in addition to the rate of freezing, the degree of C-O isotope fractionation is also controlled by the attainment of calcite saturation. However, when the rate of freezing is increased, the amount of C-O isotope fractionation between calcite and water results in strong C-O isotope disequilibrium, producing calcite with high stable C-O isotope composition (Clark and Lauriol, 1992). Therefore, the chemical processes and the rate at which they occur in the calcite-water-gas system play an important role in determining the stable C-O isotope composition and crystal habits of cryogenic carbonates.

In freezing caves, cryogenic carbonate precipitates are commonly observed on the surface of perennial/seasonal ice formations (i.e., ice plugs, stalagmites, and stalactites) as cryptocrystalline carbonate powders, or on the floor of freezing caves as loose calcite pearls or carbonate powders (e.g., Clark and Lauriol, 1992; Zak et al., 2004). In this study, we (1) examine the geochemical and stable O-H isotope composition of the various types of seasonal ice formations in Caverne de l'Ours (Québec, Canada), a thermally-responsive cave, and (2) analyze the mineralogy (XRD), micro-morphologies (SEM) and stable C-O isotope composition of the cryogenic carbonate powders associated with the formation of the various ice formations. We also document a new type of carbonate discovered in Caverne de l'Ours, spider silk calcite. The micro-morphologies of the cryogenic calcite powders were examined under cryogenic conditions and at room temperature to determine the potential presence of calcite polymorphs (vaterite or ikaite), which have shown characteristic crystal habits (e.g., Omelon et al., 2001; Grasby, 2003). To further understand the conditions and processes under which the cryogenic cave calcite precipitated, their micro-morphologies and stable C-O isotope composition are compared to those related to aufeis. Aufeis, which are sheet-like masses of horizontally layered ice that accumulate on river channels by successive overflow of perennial groundwater fed springs upon exposure to cold temperature, contain various cryptocrystalline powders, including calcite, vaterite and ikaite, within the individual ice layers. Consequently cryogenic aufeis and cave calcite powders are the only known types of cryogenic calcite precipitating as cryptocrystalline powders.

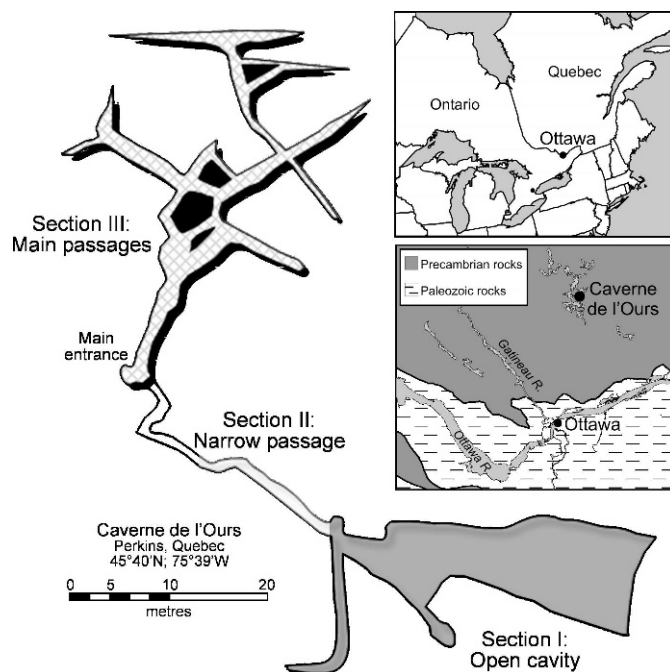


**Figure 1. Location and topography of Caverne de l'Ours (QC, Canada). The seasonal ice formations and associated cryogenic carbonates were collected in the open cavity (section I). Moonmilk deposits are found in the main passages (section III).**

#### CAVERNE DE L'OURS

##### SITE DESCRIPTION

Caverne de l'Ours (45°40'N; 75°39'W) is located in the Ottawa valley region on Precambrian Grenville marble outcrop and near the eastern limit of the Canadian Shield (Fig. 1). The cave is located in a region characterized by large seasonal temperature variations and relatively high precipitation. The mean annual air temperature  $T$  (1970–2000) recorded at the Ottawa meteorological station is  $6.0 \pm 0.8$  °C (January mean  $T$ :  $-10.8 \pm 2.9$  °C; July mean  $T$ :  $20.9 \pm 1.1$  °C), and the area receives a total of 945 mm of precipitation annually, of which one-third falls as snow (Environment Canada, 2004). The vegetation surrounding the cave consists of a mixed-deciduous forest composed of spruce (*Picea*), hemlock (*Tsuga*), cedar (*Thuja*), birch (*Betula*), and maple (*Acer*), which is characteristic of the middle Ottawa zone of the Great Lakes – St. Lawrence forest region (Rowe, 1972). The soil overlying the cave consists of a slightly acidic organic matter and plant litter (pH of 4.5), typical of soils covered by a deciduous forest (Hagen-Thorn et al., 2004). The  $p\text{CO}_2$  in the soil is approximately  $10^{-3.3}$  to  $10^{-3.1}$  ppmV in July and decreases to  $10^{-3.5}$  to  $10^{-3.4}$  ppmV in January, reflecting the biological activity of the overlying vegetation.

The age of formation of Caverne de l'Ours is unknown, but given the absence of glacial sediments inside the cave, it was probably initially scoured into the Precambrian

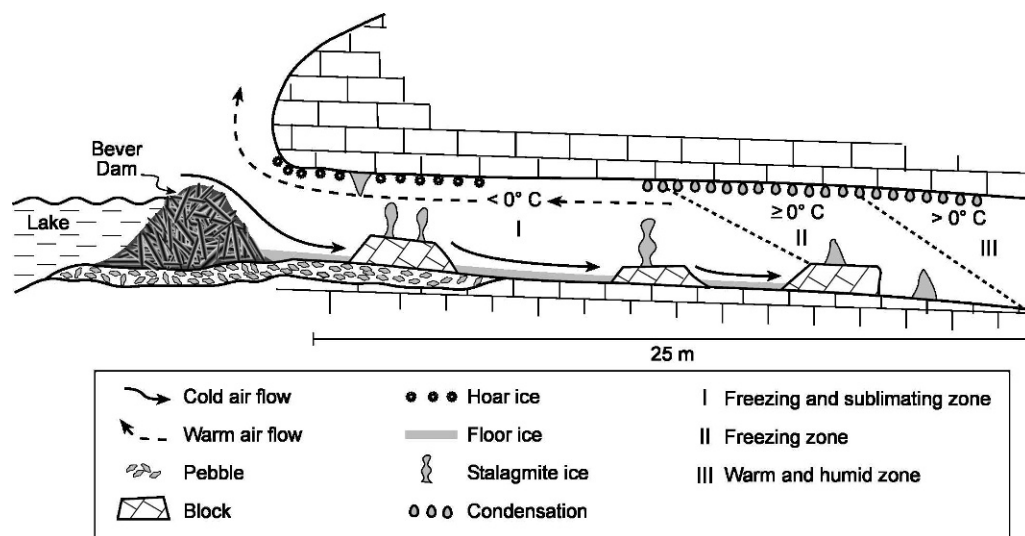


**Figure 2.** Schematic diagram illustrating the micro-climatic zones in the open cavity in Caverne de l'Ours, QC, Canada, in relation to the various types of seasonal ice formations.

Grenville marble outcrop by subglacial meltwater flowing from the Laurentide ice sheet. The Grenville marble, which consists of metamorphosed limestone ( $\text{CaCO}_3 > 95\%$ ;  $\delta^{18}\text{O} = -7.9\text{‰}$ ;  $\delta^{13}\text{C} = 2.3\text{‰}$ ) (Kretz, 1980, 2001), is highly soluble and contains numerous inclusions of quartz, gabbro, garnet and feldspar (Dresser and Denis, 1946; Prévost and Lauriol, 1994).

Caverne de l'Ours, which measures up to 280 m in length, is divided into three sections: (1) a large open cavity measuring 30-m-long and 5-m-wide; (2) the main underground section consisting of 250 m of narrow sub-horizontal passages; and (3) a 30-m-long and very narrow passage that connects the open cavity to the main underground passages (Fig. 1). The open cavity and main passages both reach a few meters in height. There is a small closed-basin lake adjacent to the entrance of the open cavity, and the presence of a beaver dam prevents the lake water from filling most of the open cavity. However, the beaver dam allows for a small stream to flow (ca.  $4\text{--}5\text{ L s}^{-1}$ ) along the floor of the open cavity, and the stream reaches the main passages of the cave through a narrow network of fissures. Near the entrance of the cavity, the stream partially freezes during winter, but it remains unfrozen (stream temperature near  $4\text{ °C}$ ) at the end of the cavity. The cryogenic cave calcite deposits discussed in this study are only found in the open cavity; inside the remainder of the cave, moonmilk is the dominant type of speleothem, although a few Holocene-age flowstones are also present (Lacelle et al., 2004).

#### MICROCLIMATE, SEASONAL ICE DISTRIBUTION AND CRYOGENIC CALCITE POWDERS

The microclimate inside the main underground passages of the cave was described in Lacelle et al. (2004), and it was found that the seasonal air temperature and relative

humidity fluctuated between  $5\text{--}15\text{ °C}$  and  $85\text{--}100\%$ , respectively. However, the microclimate in the open cavity tends to reflect that of the outside air temperature. January air temperatures range from  $-10\text{ °C}$  near the entrance, to near  $0\text{ °C}$  at the end of the cavity. Therefore, the cold dense air that enters the cavity in winter circulates along the floor. As it progresses in the open cavity, the air warms up, rises, and flows back towards the entrance along the roof (Fig. 2). The distribution of ice formations in the cavity is in part controlled by the winter  $0\text{ °C}$  isotherm, which extends to approximately 20 m inside the cavity.

In Caverne de l'Ours, as in most freezing caves in Canada (Ford and Williams, 2007), the seasonal ice formations formed either by the: (1) freezing of dripping water (ice stalagmite and stalactite), (2) freezing of stagnant or slow moving water (floor ice and curtain ice), or (3) condensation of water vapor (hoar ice) (Fig. 3). Figure 2 presents the various forms of seasonal cave ice formations in relation to the microclimatic zones in the cavity. Within the first 5 m from the entrance, a few small ice stalagmites (5- to 15-cm-high) are found on the limestone blocks, and the ceiling is covered by hoar ice. Between 5 and 10 m from the entrance, the ice stalagmites, shaped as inverse bowling pins, are more abundant and measure up to 1-m-high and 20-cm-wide. Numerous ice stalactites are also present in this section. The stalactites have a conical shape that tapers at their tips and measure up to 1-m-long. These two types of ice formations, which are formed from the freezing of dripping water, grow more rapidly when the air temperatures in the cavity are very cold, whereas when the air temperatures are slightly below  $0\text{ °C}$ , the dripping water slowly circulates on their surface, resulting in a thickening of the ice formations. In this middle section (5 to 10 m) and near the entrance of the cavity, the shapes of the ice stalagmites and stalactites are not only controlled by the

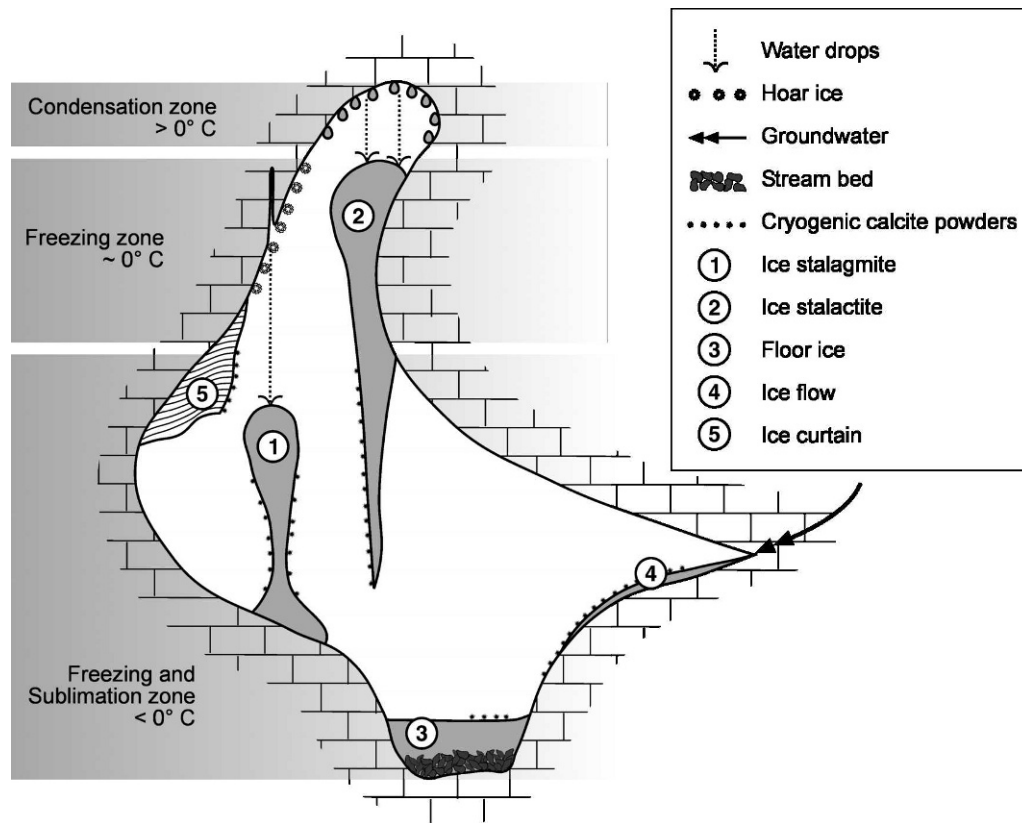


**Figure 3.** Schematic diagram of various types of seasonal ice formations encountered in the open cavity in Caverne de l'Ours, QC, Canada.

freezing of dripping water, but also by sublimation of the ice surfaces. This process lies in the equilibrium between temperature and humidity differences between the air and the ice formations. The cold and dry air that enters the open cavity flows around the ice stalagmites and stalactites, and the interaction of the water molecules at the boundary layer between the ice and air masses causes a transfer (removal) of ice to the air. Also found in the middle section of the cavity is hoar ice along the roof and curtain ice growing perpendicular on the upper walls. Further away from the entrance (10 to 20 m), the ice stalagmites have a tubular form and measure up to 1.2-m-high, indicating that sublimation is no longer active in the farthest section. Ice stalactites and hoar ice are absent in this section because the air temperature along the roof is greater than 0 °C, except on very cold winter days. Throughout the open cavity (except near the end), the floor is covered by ice. This ice forms by the freezing of lake water passing beneath the beaver dam in winter. Near the entrance, the floor ice measures 25-cm-thick, and is composed of candle ice crystals up to 5-cm-long. These characteristics approach those of aufeis, and as such, the formation of the floor ice resembles that of aufeis in the Arctic, albeit at a much smaller scale (discussed further in text).

Cryogenic calcite powders, which form during the freezing of a solution containing dissolved calcium and bicarbonate solutes, are visible on the surface on the floor ice and also on the sublimated sections of the ice stalagmites and stalactites. Deeper in the open cavity, where the ice formations are not modified by sublimation, no calcite powders are found on their surface; however, it should be noted that the melting of ice stalagmites growing deeper in the cave also released calcite powders. The cryogenic calcite powders have a whitish to yellowish color and become progressively thicker on the ice surfaces as the winter months advance, with maximum accumulations reaching 1–2 mm in March.

Calcite powders are not only found on the surface of ice formations, but also were observed on spider webs attached to the tips of the small ice stalagmites growing at the entrance of the cavity. In the literature, this type of calcite is rarely documented, but Murase et al. (2001) named it spider silk calcite, following their discovery in a laboratory experiment. The only spider species observed in the summer in the entrance of Caverne de l'Ours was *Meta ovalis*, and this species is the most common spider living in the entrance of caves in North America (Dondale et al., 2003). The spider silk has a strong ability for water condensation; and therefore, the condensation and subse-



quent freezing of water vapor containing cave aerosols on the spider silk could produce cryogenic spider silk calcite, assuming the cave aerosols contain some dissolved calcium and bicarbonate species.

## FIELD SAMPLING AND ANALYTICAL PROCEDURES

### CAVE ICE

In the winters of 2006–2007, various types of seasonal cave ice formations (hoar, curtain, floor, stalagmite, and stalactite ice) found in the open cavity of Caverne de l'Ours were collected for geochemical and stable O-H isotopes. Since the hoar and curtain ice could readily be broken off, they were collected and transferred directly into sealed plastic bags, whereas the floor ice was sampled using an ice axe and then transferred into sealed plastic bags. Near the entrance of the cavity, an entire ice stalagmite (50 cm) and stalactite (80 cm) were broken off from their limestone block and ceiling, respectively, and brought back to the laboratory in a thermally insulated box. Water dripping from the ceiling in the open cavity was also collected during the months of October and December 2006 and April 2007 in glass amber bottles for geochemical and stable O-H-C isotope measurements.

Prior to geochemical and stable O-H isotope analyses, all ice samples were melted in the laboratory, filtered through 0.45  $\mu\text{m}$  pore diameter filters, and transferred in 20 ml pre-rinsed polyethylene bottles. However, the ice stalagmite and stalactite were sectioned with a pre-cleaned saw into 2-cm-thick slices along their growth axis to verify the chemical and stable isotope (O-H) variations during their accretion. The pH of the melted ice samples, which represents an equilibrium value between the water and potentially any dissolved cryogenic calcite under the laboratory partial pressure of  $\text{CO}_2$ , was determined using a Fisher Accumet 610A pH meter calibrated with pH 4 and 7 buffer solutions. Major cations ( $\text{Ca}^{2+}$ ,  $\text{Mg}^{2+}$ ,  $\text{Na}^+$  and  $\text{K}^+$ ) were analyzed and acidified to pH 2 using ultra-pure nitric acid by Inductively Coupled Plasma Atomic Emission Spectroscopy (ICP-AES). All samples were run in duplicate at the University of Ottawa (Department of Earth Sciences) and the analytical reproducibility was  $\pm 5\%$ .

The  $^{18}\text{O}/^{16}\text{O}$  ratio of the melted ice samples was determined on  $\text{CO}_2$  equilibrated with the water at 25  $^\circ\text{C}$ . The D/H ratio was measured on  $\text{H}_2$  isotopically equilibrated with the water at 25  $^\circ\text{C}$  using a Pt based catalyst. Both stable isotope measurements were made on the same sample using a Gas Bench II interfaced with a Finnigan Mat Delta<sup>+</sup> XP isotope mass spectrometer at the G.G. Hatch Laboratory (University of Ottawa). Results are presented using the  $\delta$ -notation, where  $\delta$  represents the parts per thousand difference of  $^{18}\text{O}/^{16}\text{O}$  or D/H in a sample with respect to Vienna Standard Mean Ocean Water (VSMOW). Analytical reproducibility was of  $\pm 0.1\text{‰}$  for  $\delta^{18}\text{O}$  and  $\pm 1.5\text{‰}$  for  $\delta\text{D}$ .

### CRYOGENIC CAVE CALCITE

The mineral composition of the cryogenic carbonate deposits, identified as calcite in all cases, was determined a few months after collection. The samples were powdered, mixed with acetone and spread over a glass slide and analyzed using a Phillips PW-1800 x-ray diffractometer with a step size of 0.02 and scanning speed of 0.4 seconds per step to record the x-ray diffraction spectra.

The cryogenic calcite powders were also collected from the ice formations using different methods and examined under scanning electron microscope (SEM) either under cryogenic or room temperature conditions to verify the effect of post-field storing on their micro-morphologies and to determine the potential presence of calcite polymorphs. Four methods were used:

- (1) Cryogenic calcite powders were collected directly from the surface of the ice formations, placed in sterile roll-top plastic bags and kept at room temperature until analyzed under SEM.
- (2) Cryogenic calcite powders were collected along with the ice on which they rested, stored, and analyzed using a SEM under cryogenic conditions to verify the undisturbed micro-morphologies.
- (3) The third method consisted of collecting a section of ice stalagmite that was melted in a glass beaker back in the laboratory. The calcite powders were retrieved from the beaker after the water had completely evaporated and then examined under SEM at room temperature.
- (4) For the final method, an ice stalagmite was sectioned into small blocks, placed in a beaker covered by an aluminum sheet and desiccated (1 atm and temperature of  $-5\text{ }^\circ\text{C}$ ) in a commercial dessicator (Lab-conco Freezone) at the Geological Survey of Canada. The residual calcite powders were collected from the beaker and kept at sub-freezing temperature until SEM examination under cryogenic conditions.

Calcite powders were also collected from the spider webs attached on the small ice stalagmites near the entrance of the cavity to examine the morphology of the crystals. The cryogenic spider silk calcite was collected directly on a carbon tape mounted onto an aluminum stub and kept at sub-freezing temperature until examination under SEM. Prior to examination under SEM, all calcite powders (except for the powder collected with the ice substrate, which was put directly uncovered onto an aluminum stub) were mounted onto an aluminum stub using doubled-sided carbon tape and then sputter-coated with gold for 60 seconds. The micro-morphologies of calcite precipitates were examined using a JEOL 6400 SEM at the Université du Québec à Montréal.

The  $^{18}\text{O}/^{16}\text{O}$  and  $^{13}\text{C}/^{12}\text{C}$  ratios of the cryogenic cave calcite powders were determined on  $\text{CO}_2$  gas produced by reacting the powdered calcite with 100% phosphoric acid ( $\text{H}_3\text{PO}_4$ ) in glass septum vials for 24 hours at 25  $^\circ\text{C}$ . The

evolved CO<sub>2</sub> gas was analyzed in continuous flow using a Gas Bench II interfaced with a Finnigan Mat Delta<sup>+</sup> XP isotope mass spectrometer at the G.G. Hatch Isotope Laboratory, University of Ottawa. Stable isotope data for C and O are expressed in  $\delta$ -notation, where  $\delta$  represents the parts per thousand difference of <sup>13</sup>C/<sup>12</sup>C and <sup>18</sup>O/<sup>16</sup>O in a sample with respect to the Vienna Pee-Dee Belemnite standard (VPDB). Analytical reproducibility is  $\pm 0.15\text{‰}$  for both isotopes.

## RESULTS

### CAVE ICE FORMATIONS

The geochemical and stable O-H isotope compositions of the various seasonal cave ice formations in Caverne de l'Ours are presented in Figures 4 and 5. The ice formations have similar geochemical and isotopic compositions: a pH ranging between 7 and 8, a Ca<sup>2+</sup> concentration averaging  $15.9 \pm 6.7 \text{ mg L}^{-1}$ , typical of karst water in the area (Prévost and Lauriol, 1994), and  $\delta^{18}\text{O}$  and  $\delta\text{D}$  values averaging  $-8.2 \pm 0.2\text{‰}$  and  $-57.6 \pm 2.8\text{‰}$ , respectively (Fig. 4A). Although the  $\delta^{18}\text{O}$  compositions of the ice stalagmite, ice stalactite, curtain and hoar ice are similar, separate regression lines are obtained in a  $\delta\text{D} - \delta^{18}\text{O}$  diagram. Individual regression slopes of 5.1 ( $\delta\text{D} = 5.1 \delta^{18}\text{O} - 16.2$ ;  $R^2 = 0.58$ ), 5.6 ( $\delta\text{D} = 5.6 \delta^{18}\text{O} - 11.1$ ;  $R^2 = 0.57$ ), and 2.7 ( $\delta\text{D} = 2.7 \delta^{18}\text{O} - 37.6$ ;  $R^2 = 0.40$ ) are calculated for the ice stalactite, ice stalagmite, and ice curtain, respectively (Fig. 4B), suggesting potentially unique mechanism of formation for each type of ice.

Sampling along the growth axis of the ice stalactite and stalagmite revealed slight geochemical and isotopic variations related to their separate accretion processes (Fig. 5). In the 80-cm-long ice stalactite, the pH increases from 6.8 at the base to 7.3 at its tip. The geochemical composition of the ice stalactite is dominated by Ca<sup>2+</sup> ( $14 \pm 2.3 \text{ mg L}^{-1}$ ), followed by Na<sup>+</sup> ( $1.7 \pm 0.9 \text{ mg L}^{-1}$ ) and K<sup>+</sup> ( $1.2 \pm 0.8 \text{ mg L}^{-1}$ ), but their concentrations do not show any trends from the base to the summit. It is interesting to observe that the concentrations of K<sup>+</sup> and Na<sup>+</sup> fluctuate together, whereas the variation in the concentration of Ca<sup>2+</sup> is independent. The source of K<sup>+</sup> and Na<sup>+</sup> is probably related to some clastic component, which can be either clay transported together by the drip water or cave aerosols deposited on the wet surface of the ice stalactite. The  $\delta^{18}\text{O}$  composition of the ice stalactite shows a progressive depletion trend from  $-7.1\text{‰}$  at its base to  $-8.7\text{‰}$  at its tip.

In the 50-cm-long ice stalagmite, the pH also progressively increases as it grew, ranging from 6.9 at the base to 7.9 at its tip. The K<sup>+</sup> and Na<sup>+</sup> concentration in the ice stalagmite is similar to that of the stalactite. However, the Ca<sup>2+</sup> solutes concentration reaches a much greater concentration (up to  $47.2 \text{ mg L}^{-1}$ ). Like the ice stalactite, the solute concentrations in the stalagmite do not show any trends during ice accretion (Fig. 5). The  $\delta^{18}\text{O}$  of the ice stalagmite varies between  $-7.9$  and  $-8.9\text{‰}$ . It was

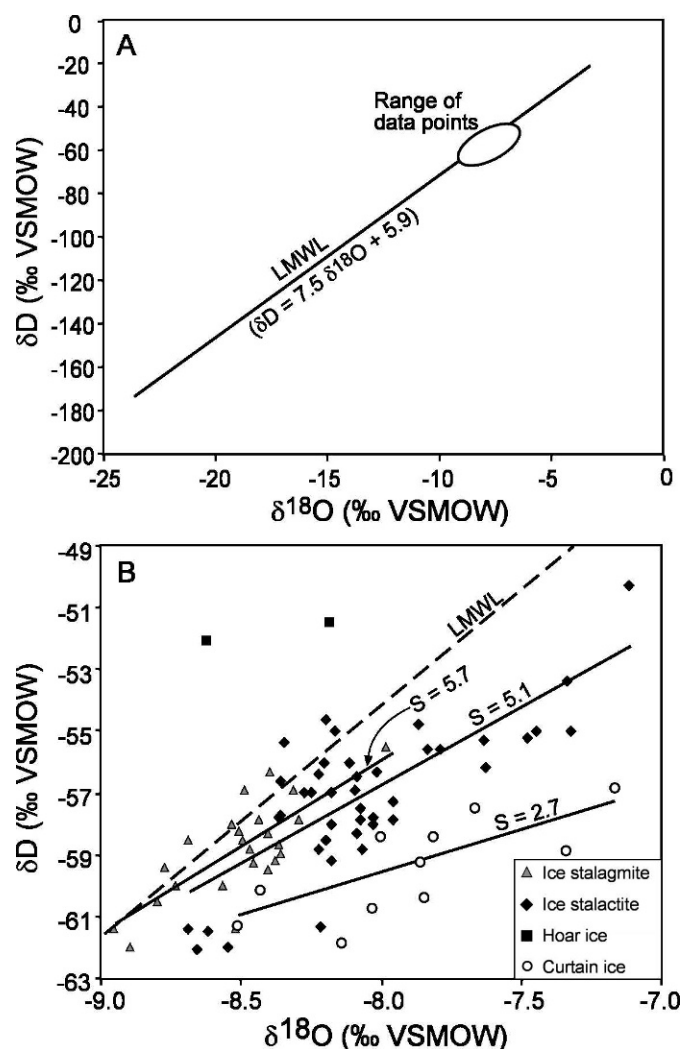


**Figure 4.** A) Range of stable O-H isotope composition of seasonal ice formations in Caverne de l'Ours, QC, Canada, compared to that of the seasonal precipitation recorded in Ottawa, which is defined by the Local Meteoric Water Line (LMWL:  $\delta\text{D} = 7.5 \delta^{18}\text{O} + 5.9$ ; IAEA/WMO, 2004). B) Stable O-H isotope composition of seasonal ice formations (ice stalagmite, ice stalactite, hoar ice and curtain ice) in Caverne de l'Ours and their respective regression line (S).

interesting to observe that once thawed, the color of the water of the ice stalagmite and stalactite was yellowish, suggesting the presence of amino acids. In fact, the cave drip water has a measured dissolved organic content (DOC) ranging from  $4.1$  to  $6.9 \text{ mg L}^{-1}$  (unpublished data).

### CRYOGENIC CAVE CALCITE POWDERS

The  $\delta^{18}\text{O}$  and  $\delta^{13}\text{C}$  composition of the cryogenic calcite powders is presented in Figure 6. The stable isotopic composition of the cryogenic calcite powders is invariant of the cave ice formation from which they were collected and

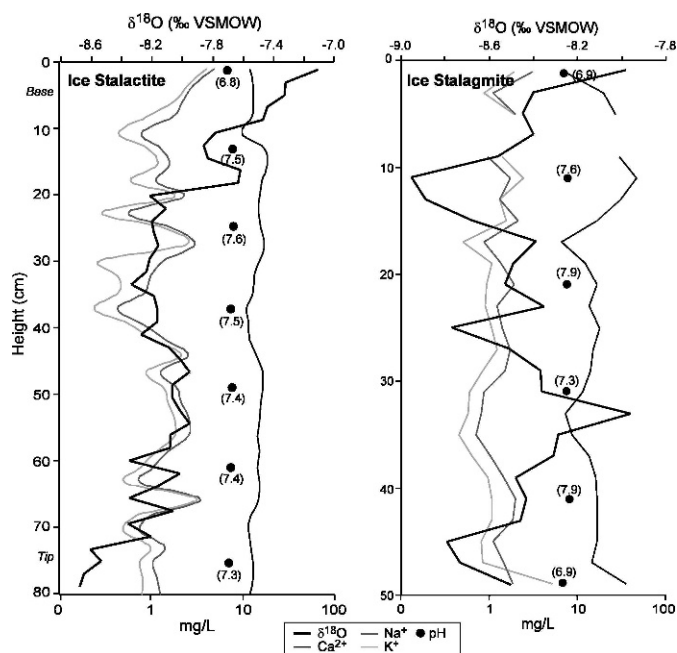


**Figure 5.** Geochemical ( $\text{Ca}^{2+}$ ,  $\text{Na}^{+}$ ,  $\text{K}^{+}$  and pH) and  $\delta^{18}\text{O}$  composition along growth axis of an ice stalactite and ice stalagmite found in the open cavity in Caverne de l'Ours, QC, Canada.

of the post-sampling handling. The cryogenic calcite powders all have  $\delta^{18}\text{O}$  values ranging from  $-11.3$  to  $-3.7$ ‰ and  $\delta^{13}\text{C}$  values between  $5.8$  and  $11.9$ ‰, which are among the most positive values in the literature. The  $\delta^{18}\text{O}$  and  $\delta^{13}\text{C}$  of calcite powders collected from the sublimated ice stalagmite fall also within this isotopic range. Cryogenic calcite powders collected from the surface of floor ice in the nearby Lusk cave ( $45^{\circ}39'\text{N}$ ;  $75^{\circ}38'\text{W}$ ) yielded very similar  $\delta^{18}\text{O}$  and  $\delta^{13}\text{C}$  values (Clark and Lauriol, 1992).

Unlike the  $\delta^{18}\text{O}$  and  $\delta^{13}\text{C}$  values, the cryogenic calcite powders produced varied crystal arrangements depending on the post-sampling storage and analytical methods (room or sub-freezing temperature) during examination under SEM (Figs. 7 and 8). The crystal arrangement of the first group of cryogenic calcite powders, which were collected from the surface of the ice stalagmites and stalactites and stored at room temperature prior to analysis, is composed of  $3\text{--}8\text{ }\mu\text{m}$  rhombohedral crystals (Fig. 7A–C). The surface of the calcite crystals is often pitted and their edges are etched, suggesting calcite disintegration after precipitation by local dissolution. In contrast, the cryogenic calcite powders analyzed directly from the surface of the ice and those collected from sublimated ice stalagmites under cryogenic conditions showed crystal habits different from the first group (Fig. 8). These calcite crystals are composed of spheres ranging from  $<1$  to  $2\text{ }\mu\text{m}$  in diameter and thick calcite

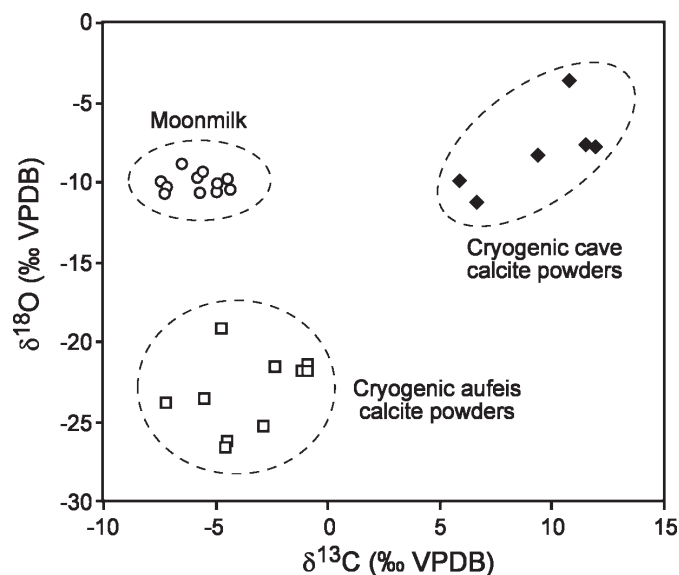


**Figure 6.** Stable C-O isotope composition of cryogenic calcite powders found on the surface of the various seasonal ice formations in Caverne de l'Ours. Also shown for comparison purposes is the  $\delta^{13}\text{C}$  and  $\delta^{18}\text{O}$  composition of moonmilk found in the main passages of Caverne de l'Ours (Fig. 1), and cryogenic aufeis calcite powders (sampled from limestone terrain in the northern Yukon, Canada), the only other known type of cryogenic calcite precipitating as cryptocrystalline powders.  $\delta^{13}\text{C}$  and  $\delta^{18}\text{O}$  data for moonmilk and cryogenic aufeis calcite powders derived from Lacelle et al. (2004) and Clark and Lauriol (1997), respectively.

needles up to  $20\text{ }\mu\text{m}$  long. In some instances, several spheres aggregate together, producing a chain-like appearance (Fig. 8B, D). Finally, the cryogenic calcite powders analyzed from evaporated melted ice stalagmites and stalactites are composed of  $3\text{--}10\text{ }\mu\text{m}$  rhombohedral crystals that are often stacked together (Fig. 7D–F). The surface of the crystals is smooth, but their edges are etched, similar to the first group of calcite powders (collected from the surface of the ice formations and kept at room temperature prior to analysis). Overall, none of these crystal habits resemble that of ikaite, which is typically composed of anhydrous calcite crystals (Omelson et al., 2001). However, the spherical-shaped crystal aggregates observed under cryogenic conditions closely resemble those of vaterite precipitated under natural and laboratory setting (e.g., Turnbull, 1973; Fairchild et al., 1996; Vecht and Ireland, 2000; Grasby, 2003).

The spider silk calcite produced a unique crystal habit (Fig. 9). The calcite attached to the spider's silk showed elongated crystals up to  $3\text{ }\mu\text{m}$  long that formed clusters less than  $10\text{ }\mu\text{m}$  wide along the spider's silk (Fig. 9 C–F). These dimensions of single clusters are probably constrained by the weight of the calcite crystals on the silk.



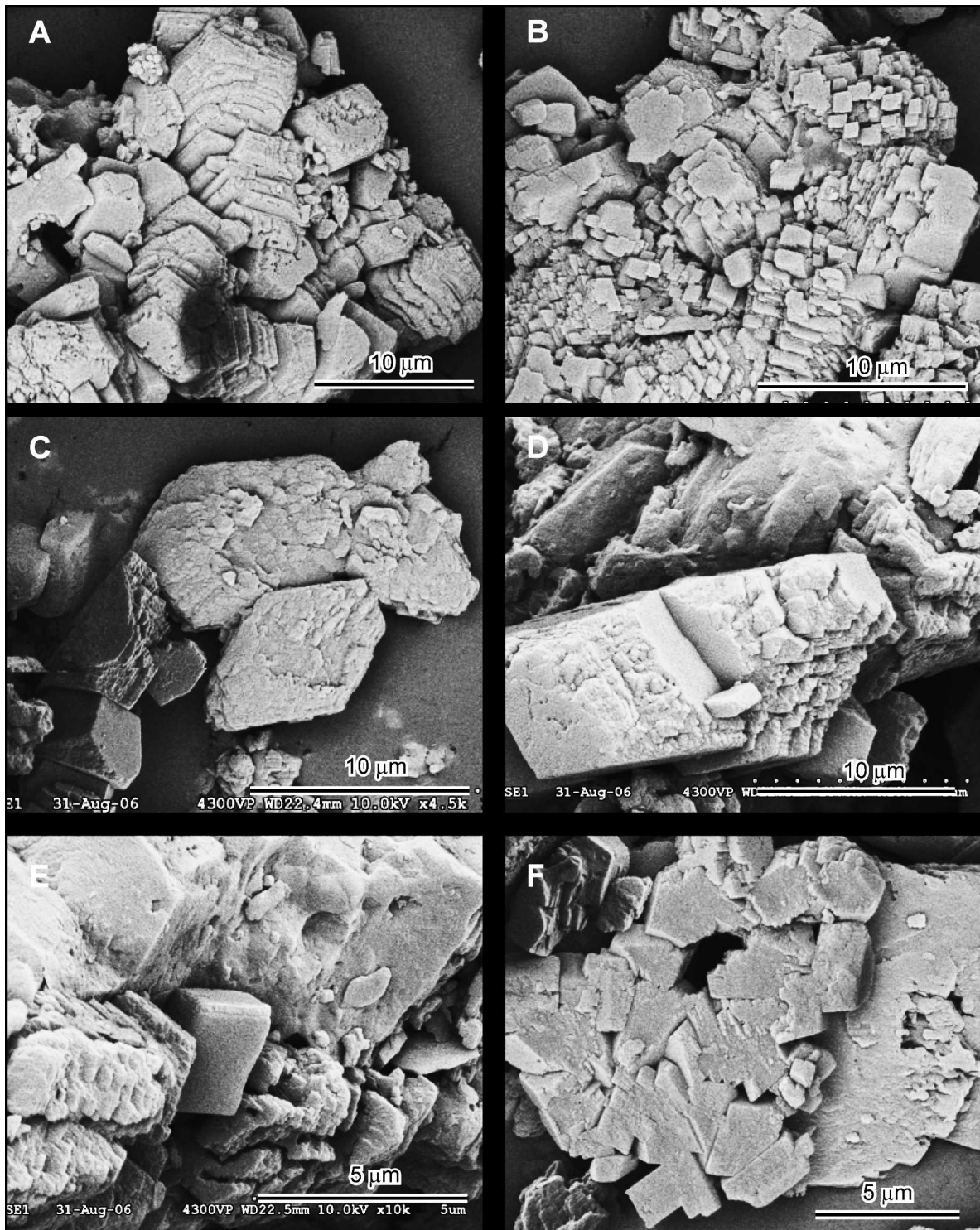


**Figure 7.** Secondary electron images of cryogenic calcite powders collected on the surface of various ice formations in Caverne de l'Ours. The images were acquired at room temperature with a SEM. A–C) cryogenic calcite powders collected from the surface of ice stalagmites and stalactites; and D–F) calcite powders recovered from a beaker in which a section of ice stalagmite was melted and left to evaporate in the laboratory.



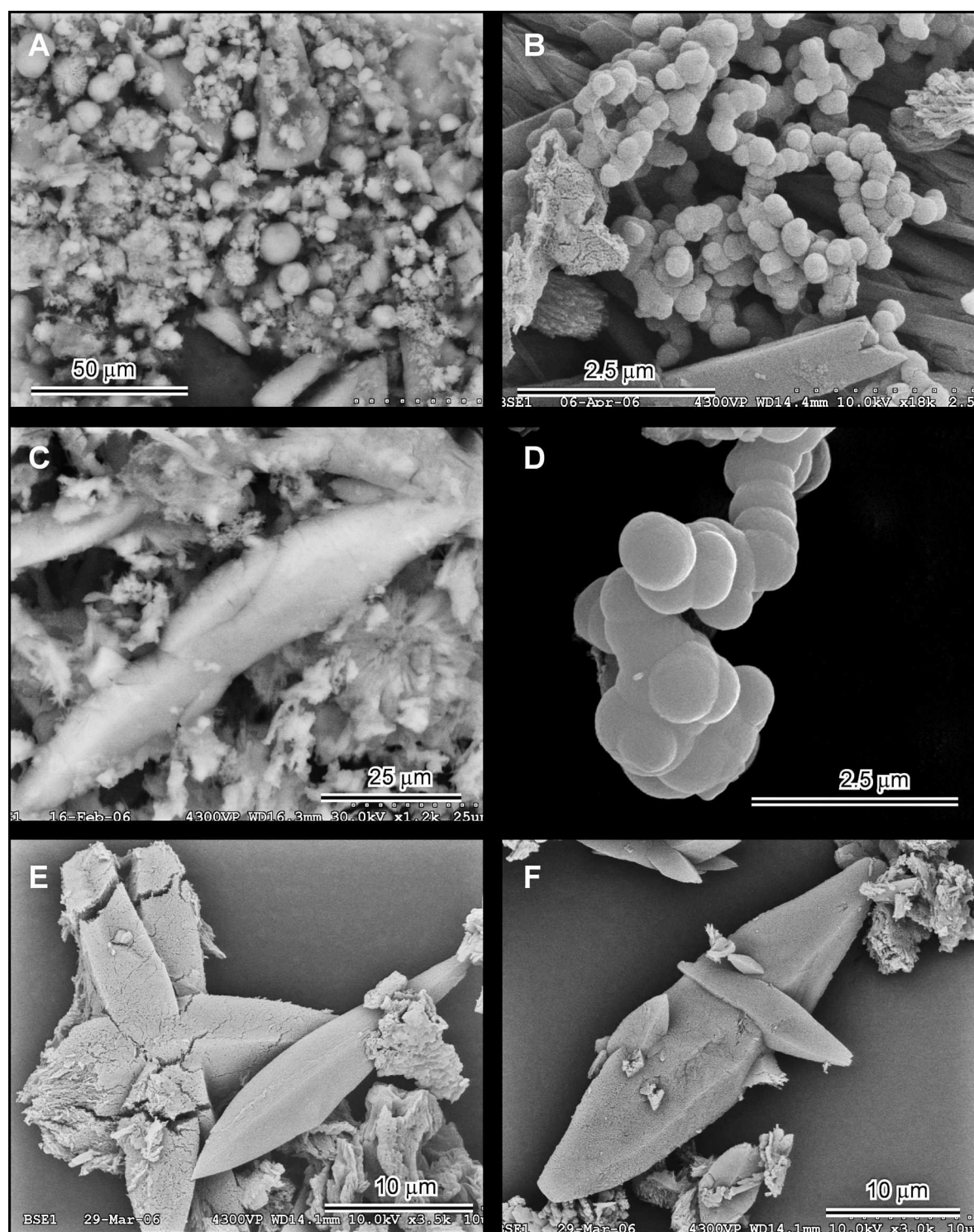


**Figure 8.** Secondary electron images of cryogenic calcite powders collected on the surface of various ice formations in Caverne de l'Ours. The images were acquired at sub-freezing temperature with a SEM. A–C) cryogenic calcite powders collected from the surface of ice stalagmite using cryogenic sample transport and analysis; and D–F) calcite powders recovered from a beaker in which a section of ice stalagmite was sublimated in the laboratory under cryogenic condition, transport, and analysis.

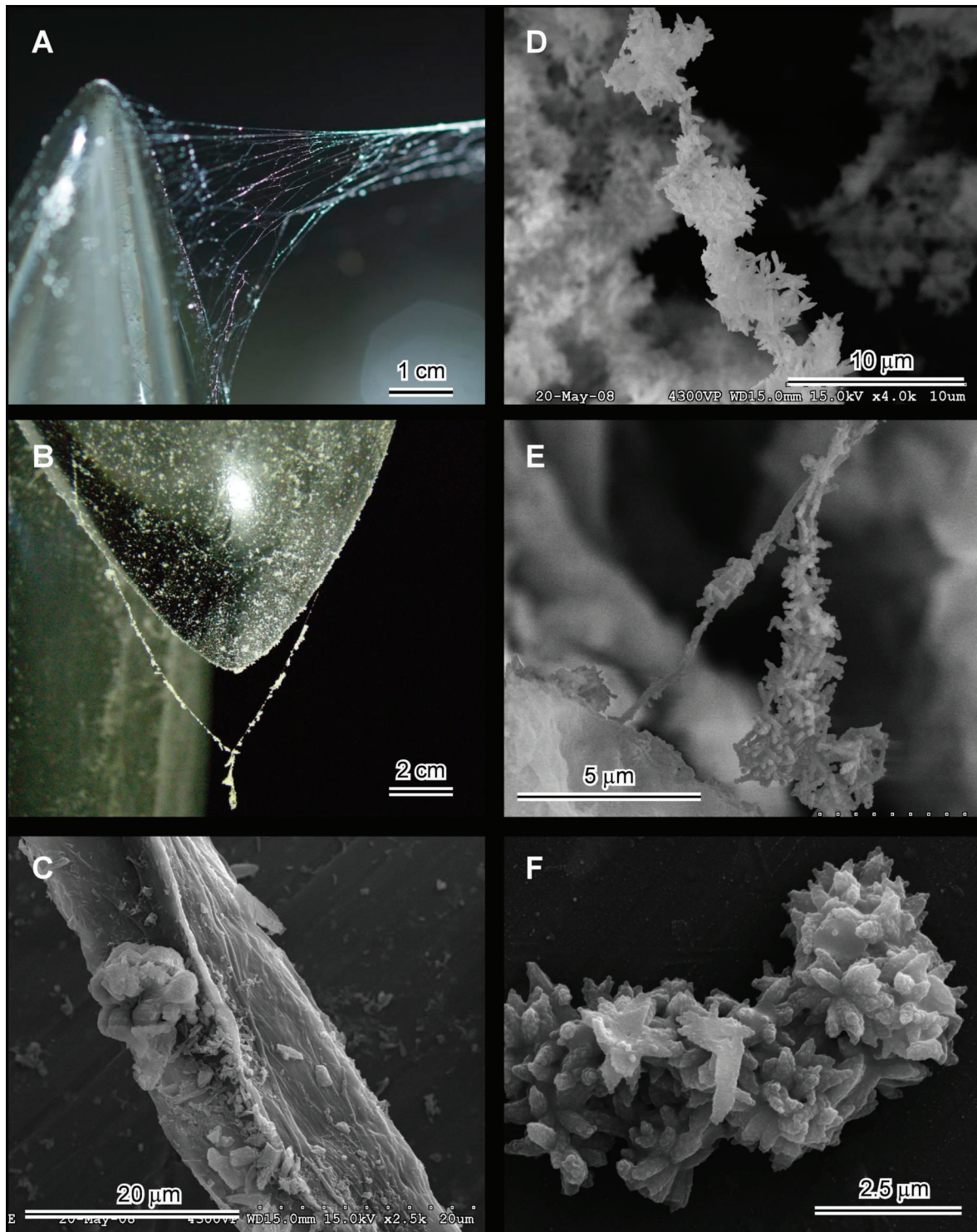


**Figure 9.** A–B) Field photographs of calcite powders on spider silk attached to a small ice stalagmite near the entrance of the open cavity of Caverne de l'Ours. C–F) Secondary electron images of spider silk calcite acquired at room temperature with a SEM.



## DISCUSSION

### ORIGIN OF THE SEASONAL CAVE ICE FORMATIONS: EVIDENCE FOR KINETIC ISOTOPE EFFECTS

The formation of the seasonal cave ice formations examined in this study is well known in the literature (i.e., Ford and Williams, 2007) and it has been described here in a previous section. However, little is known regarding the degree of isotope equilibrium/disequilibrium during the formation of the hoar, curtain, stalagmite and stalactite ice bodies. Such information can be provided by examining the  $\delta D$ – $\delta^{18}O$  relation in the ice formations (Fig. 4). During equilibrium freezing, the ice samples are aligned along a regression line that will be lower than the local meteoric water line (LMWL;  $\delta D = 7.5 \delta^{18}O + 5.9$ ;  $R^2 = 0.97$ ; IAEA/WMO, 2004) because the amount of incorporation of the heavier isotopes in the ice (D and  $^{18}O$ ), which follows a Rayleigh-type fractionation, is slightly different for both isotopes (Jouzel and Souchez, 1982; Souchez and Jouzel, 1984). According to Jouzel and Souchez (1982), the slope of the freezing line depends mainly on the initial isotopic composition of the water, with the more depleted waters having a lower slope value. The conditions prevailing during freezing (open versus closed system), and the rate of supply of water to the freezing fronts, have little effect on the freezing slope (Souchez and Jouzel, 1984). Based on the Jouzel and Souchez (1982) model and using an initial water  $\delta^{18}O$  and  $\delta D$  values of  $-11.4\text{‰}$  and  $-78.8\text{‰}$ , respectively, and the average annual precipitation values in Ottawa (IAEA/WMO, 2004), the ice formations in the cave resulting from equilibrium freezing should plot along a slope of 5.9.

Another parameter that provides clues into the rate of freezing during the formation of ice bodies is the  $d$  –  $\delta D$  relation, where  $d$  represents the deuterium excess ( $d = \delta D - 8 \delta^{18}O$ ) (Dansgaard, 1961). During equilibrium freezing, the first ice that forms has a greater  $\delta D$  (and  $\delta^{18}O$ ) value due to the preferential partitioning of the D isotope in the ice (i.e., with an associated depletion of heavy isotopes in the residual water), but as freezing progresses, the  $\delta D$  values of the ice become progressively lower. This is accompanied by a concurrent increase in  $d$  values because the freezing equilibrium slope has a value lower than the LMWL. As a result, a negative relation is expected between  $d$  and  $\delta D$  during equilibrium freezing (Souchez et al., 2000).

If we examine the  $\delta D$  –  $\delta^{18}O$  and  $d$  –  $\delta D$  relations in the Caverne de l'Ours seasonal ice formations, a few key features emerge. First, all cave ice formations have  $\delta^{18}O$  and  $\delta D$  values within the range of summer precipitation and of the stream flowing inside the open cavity (Fig. 4A). Secondly, the stalagmite and stalactite ice formations lie on positive slopes that are less than the LMWL (7.5), but similar to the theoretical freezing slope (5.9) (Fig. 4B). Individual regression slopes of 5.1 ( $\delta D = 5.1 \delta^{18}O - 16.2$ ;  $R^2 = 0.58$ ) and 5.6 ( $\delta D = 5.6 \delta^{18}O - 11.1$ ;  $R^2 = 0.57$ ) are

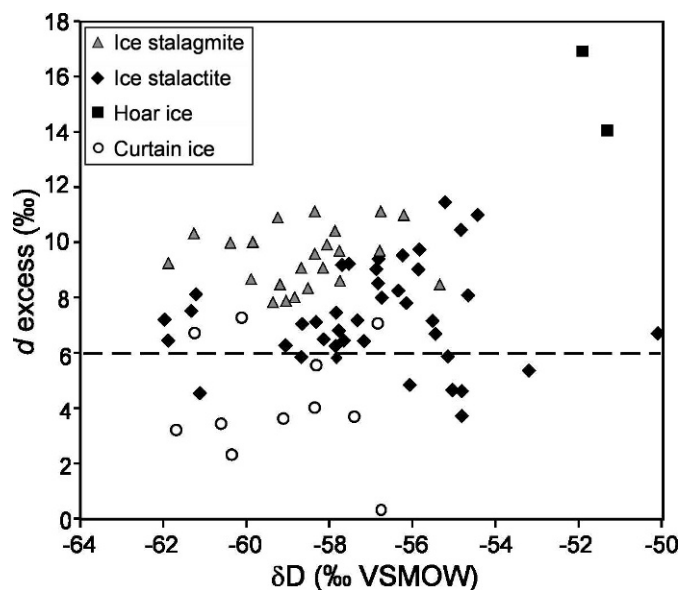


**Figure 10.** Deuterium excess ( $d$ ) and stable D isotope composition of the various seasonal ice formations in Caverne de l'Ours, QC, Canada. Horizontal dashed line represents  $d$  in local precipitation.

calculated for the ice stalactite and ice stalagmite, respectively (Fig. 4B). By contrast, the curtain ice samples plot along a regressive slope  $\delta D = 2.7 \delta^{18}O - 37.6$ ;  $R^2 = 0.40$  that is much less than the LMWL and predicted freezing slope. Thirdly, there is no negative relation between  $d$  –  $\delta D$  in all cave ice formations (Fig. 10), suggesting the non-existence of a freezing slope; or in other words, freezing occurred under non-equilibrium conditions. In fact, even though regression slopes were calculated for the various ice formations, their correlation coefficient is rather weak ( $R^2 < 0.58$ ). Finally, the hoar ice on the ceiling of the cave shows strong enrichment in D, as it plots well above the LMWL (Fig. 4B). Overall, these unusual isotopic features cannot be explained by the progressive freezing of water under equilibrium conditions, but can be attributed to kinetic isotope effects during the successive freezing of thin layers of water. The arguments in favor of non-equilibrium freezing for the formation of each seasonal ice type formations are presented below.

By definition, hoar ice forms by direct condensation of water vapor on the cold ceiling. The effect of condensation is evident in the  $\delta D$  –  $\delta^{18}O$  diagram, where the hoar ice samples plot well above the LMWL (Fig. 4B). This is attributed to the effect of air circulation dynamics inside the open cavity. The non-equilibrium evaporation of the stream inside the open cavity would produce water vapor plotting above the LMWL, followed by equilibrium condensation of the water vapor along the LMWL (Fig. 11). This process produces  $d$  values much greater than 10‰ that are increasing under decreasing relative humidity conditions. A simple calculation using the



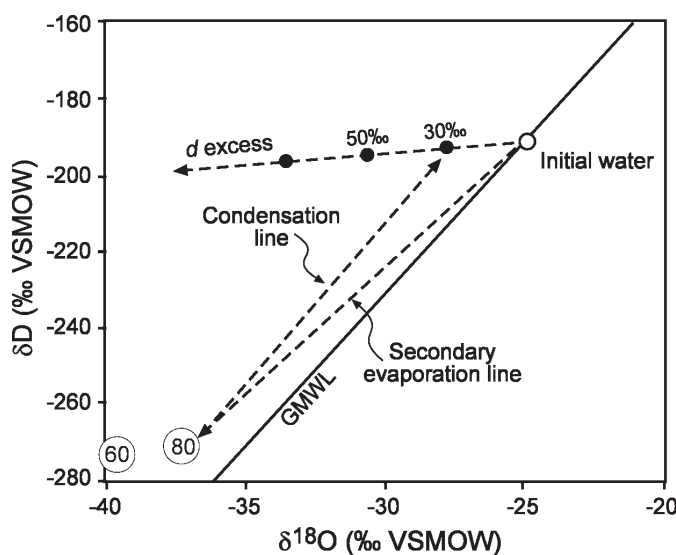


**Figure 11.**  $\delta D - \delta^{18}O$  systematic during condensation of secondary evaporated water (i.e., small stream on the floor of the open cavity). When humidity conditions are near 100%, precipitation plots close to the local meteoric water line, however, under decreasing relative humidity conditions, the vapor (evaporated water) becomes strongly depleted and precipitation formed by equilibrium condensation plots further above the GMWL (global meteoric water line) along a condensation line with a slope very similar to the GMWL.

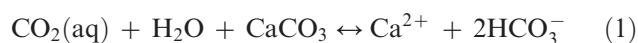
average  $\delta^{18}O$  and  $\delta D$  of the small stream in the open cavity in winter ( $-7.5 \pm 1.0\text{‰}$  and  $-56.6 \pm 2.1\text{‰}$ , respectively) (Lacelle et al., 2004), the fractionation factor between ice and vapor ( $\delta^{18}O$  ice-vapor =  $14.7\text{‰}$ ;  $\delta D$  ice-vapor =  $127\text{‰}$ , both at  $0^\circ\text{C}$ ; Majoube, 1971), and average relative humidity in winter ( $74.7\%$ ; this value is probably slightly less in the open cavity since the air becomes warmer), shows that the condensing ice would have a  $\delta^{18}O$  and  $\delta D$  composition of  $-7.9\text{‰}$  and  $-39.2\text{‰}$ , respectively, and a  $d$  excess of  $24.7\text{‰}$ . These predicted values are similar to the measured  $\delta^{18}O$ ,  $\delta D$  and  $d$  values of the hoar ice in Caverne de l'Ours (Figs. 4B and 10), indicating that the stable O-D isotope composition of hoar preserved the condensation signature.

Ice stalagmites and stalactites and ice curtains originate from the freezing of dripping water. As the  $\delta^{18}O$  values of these ice formations are within the range of summer precipitation (Fig. 4A), the percolating water in the open cavity during the winter originates from rainfall ground water stored in the overlying soil (epikarst zone), and not from snow meltwater. In the  $\delta D$  and  $\delta^{18}O$  diagram (Fig. 4B), the ice stalagmite and stalactite plot near the predicted equilibrium freezing slope of  $5.9$ , although they have a weak correlation coefficient ( $R^2 \sim 0.58$ ). However, the ice curtain plots along a much lower slope ( $\delta D = 2.7$   $\delta^{18}O - 37.6$ ). In the  $d - \delta D$  diagram, the three ice types do not show a clear relation, as they are scattered across broad

horizontal bands (Fig. 10). These observations, and the fact that no trend is displayed in the vertical distribution of heavy isotopes ( $^{18}O$  and  $D$ ) during the accretion of the ice stalagmite and stalactite (Fig. 5), indicate that they grew from the successive freezing of water dripping from the ceiling under non-equilibrium conditions. The sublimation of the ice formations by air circulation would not affect the stable O-H isotope of the remaining ice, as sublimation is a physical surface phenomenon.

#### FORMATION OF CRYOGENIC CAVE CALCITE POWDERS: A COMPARISON WITH CRYOGENIC AUFEIS CALCITE POWDERS

Cryogenic cave calcite and cryogenic aufeis calcite are the only two known types of calcite powders formed by the freezing of calcium-bicarbonate waters. In the simplest form, the formation (and dissolution) of calcite can be expressed by this reaction:



During the formation of calcite minerals under equilibrium conditions, the heavy isotopes ( $^{18}O$  and  $^{13}C$ ) are preferentially incorporated from the aqueous phase into the minerals in a proportion governed by the isotope fractionation factor, and by such, the C-O isotope composition of calcite is controlled by the  $\delta^{18}O$  and  $\delta^{13}C_{\text{DIC}}$  composition of the parent water and temperature at which precipitation occurs. However, it is well known that freezing can modify the isotope composition of the aqueous phase as the products are being isolated immediately after their formation (Rayleigh distillation), leading to a progressive depletion in  $\delta^{18}O$  and enrichment in  $\delta^{13}C_{\text{DIC}}$  in the residual water (Lacelle et al., 2006). However, it was shown in the previous section that the seasonal cave ice formations examined in this study formed through non-equilibrium (rapid) freezing of waters. Therefore, the kinetic isotope effect during the formation of the ice stalagmites and stalactites by water freezing rapidly should also create isotopic disequilibrium between the aqueous phase and the precipitating calcite, the latter showing an increase in heavy isotopes. Clark and Lauriol (1992) demonstrated that the rapid freezing of a calcium bicarbonate solution that is at or near calcite saturation led to strong C isotope disequilibrium between the precipitating calcite and the escaping  $\text{CO}_2$  ( $\epsilon^{13}C \text{ CaCO}_3\text{-CO}_2 = 31.2 \pm 3.1\text{‰}$ ) (Clark and Lauriol, 1992). By contrast, the stable O isotope fractionation between water and calcite during kinetic freezing ( $\epsilon^{18}O \text{ CaCO}_3\text{-H}_2\text{O} = 36.7 \pm 1.3\text{‰}$  VSMOW) (Clark and Lauriol 1992) is only slightly greater than equilibrium values ( $\epsilon^{18}O \text{ CaCO}_3\text{-H}_2\text{O} = 33.6\text{‰}$  VSMOW) (Kim and O'Neil, 1997). According to these kinetic isotope enrichment factors and the average  $\delta^{13}C_{\text{DIC}}$  of drip waters ( $-11.9 \pm 1.3\text{‰}$ ; unpublished data) and  $\delta^{18}O$  of the various ice formations ( $-8.2 \pm 0.2\text{‰}$  VSMOW), the

$\delta^{13}\text{C}$  ( $9.4 \pm 2.6\text{‰}$ ) and  $\delta^{18}\text{O}$  values ( $-8.9 \pm 1.6\text{‰}$  VPDB) of the cryogenic calcite powders in Caverne de l'Ours are within the range expected of a formation by kinetic freezing.

Cryogenic cave calcite powders have highly distinct  $\delta^{13}\text{C}$  and  $\delta^{18}\text{O}$  values from those measured in the cryogenic calcite powders formed in association with aufeis, the latter having much lower  $\delta^{13}\text{C}$  and  $\delta^{18}\text{O}$  values (Fig. 6). Aufeis (icings) are sheet-like masses of horizontally layered ice that form on river channels by successive freezing of overflow of perennial groundwater-fed springs upon exposure to cold air. Stable isotope profiles within the ice layers indicate that the growth of aufeis occurs under closed-system equilibrium conditions (Elver, 1994; Clark and Lauriol, 1997). As a result, unlike the seasonal cave ice formations discussed in this study, the residual water is covered by a sheet of ice that grows downwards, leading to saturation in the residual water of various minerals, including calcite ( $\text{CaCO}_3$ ) and ikaite ( $\text{CaCO}_3 \cdot 6\text{H}_2\text{O}$ ), and their precipitation within the ice (Hall, 1980; Clark and Lauriol, 1997; Heldmann et al., 2005; Lacelle et al., 2006). Accordingly, a closed system Rayleigh-type fractionation process occurs during the aggradation of aufeis. Although Jouzel and Souchez (1982) and Souchez and deGrotte (1985) demonstrated the O isotope systematics associated with the slow freezing of low ionic strength waters under equilibrium conditions, much remains to be known about the C isotope. It can be expected that the C isotope fractionation during freezing under equilibrium conditions involves a C isotope mass balance in the  $\text{CO}_2\text{-HCO}_3\text{-CO}_3\text{-CaCO}_3$  system. Considering that the DIC species ( $\text{CO}_{2\text{aq}}\text{-HCO}_3\text{-CO}_3$ ) fractionate differently among them, and that their relative concentration is set by pH, the  $\delta^{13}\text{C}_{\text{DIC}}$  and  $\delta^{13}\text{C}_{\text{CaCO}_3}$  during equilibrium freezing is not simply controlled by the initial geochemical and isotopic composition of the source water, but also by changing physical and geochemical conditions as freezing progresses (i.e., pH and evolved  $\text{CO}_2$  during the precipitation of calcite). Given the different conditions of formation for the aufeis (closed system equilibrium freezing), the cryogenic aufeis calcite powders are characterized by  $\delta^{13}\text{C}$  and  $\delta^{18}\text{O}$  values that are in equilibrium with that of the water from which they precipitated (Lacelle et al., 2006). These characteristics indicate that the limiting process affecting the degree of deviation between the stable C-O isotope composition of the cryogenic aufeis calcite (formed under equilibrium conditions) and water from which they precipitated is the attainment of calcite saturation, whereas for the cryogenic cave calcite powders (formed under kinetic conditions), it is the rate of precipitation of calcite.

#### MICROMORPHOLOGIES OF CRYOGENIC CAVE CALCITES: ABIOTIC AND PSEUDO-BIOGENIC SIGNATURES

In natural environments, such as in caves, calcite crystals commonly display a wide range of crystal micromorphologies. Although rhombohedral habit is

highly suggestive of an inorganic precipitation of calcite, the formation of spherical crystal aggregates is usually attributed to an organic influence (Folk, 1993; Braissant et al., 2003). In this study, it was shown that the cryogenic cave-calcite powders, which are produced by freezing, an abiotic process, revealed highly different crystal habits depending on the procedures used to collect the sample, and the conditions under which it was examined under SEM. The samples analyzed under room temperature all produced rhombohedral crystals (either single or stacked) (Fig. 7), whereas the ones examined under cryogenic conditions showed small spheres ( $<2\text{ }\mu\text{m}$ ) and thick needle structures (Fig. 8). Needle-like crystals are also the dominant type of crystal habit observed in cryogenic aufeis calcite (e.g., Lacelle, 2007). The samples examined under cryogenic conditions probably preserved the undisturbed nature of the calcite powders, whereas those examined at room temperature were probably altered and recrystallized before analysis. The latter effect would not greatly affect the stable C-O isotope composition of the calcite.

Considering that the formation of cryogenic carbonate powders is purely abiotic and that vaterite is stable at low temperature ( $<10\text{ }^\circ\text{C}$  and 1 atm; Albright, 1971) and precipitates in a spherical shape with crystals ranging from 0.05 to  $2\text{ }\mu\text{m}$  (Kralj et al., 1990; Vecht and Ireland, 2000), the most plausible explanation for the observation of small spheres ( $<2\text{ }\mu\text{m}$ ) in the crystal habits of the cryogenic powders is that they consist of vaterite. This metastable polymorph of calcite recrystallizes to calcite when in contact with water (Silk, 1970), which would explain why spheres were not observed in the samples examined at room temperature because they were exposed to water during melting of the ice formations. The formation of vaterite during freezing is not unusual and was also observed by Fairchild et al. (1996) during laboratory experiments, and by Grasby (2003) in spring deposits in the high Arctic. Although higher pH values (between 9.3 and 10.0; Kralj et al., 1990) than what was measured in the ice formations (Fig. 5) are necessary to precipitate vaterite, it is possible that favorable microenvironments were created within the accretion of the various annual ice formations that allowed vaterite to precipitate. Vaterite was not identified in our XRD measurements because the samples were not kept frozen for these analyses. It is therefore suggested that care should be taken before suggesting biological origin of calcite precipitates based solely on crystal habits because they might represent pseudo-biogenic structures formed through abiotic processes.

#### CONCLUSIONS

Based on the results presented in this study, the following conclusions can be reached regarding the formation of seasonal cave ices and the associated cryogenic calcite powders in Caverne de l'Ours, QC, Canada:

1. The seasonal ice formations, which either formed by (1) freezing of dripping water (ice stalagmite and stalactite); (2) freezing of stagnant or slow moving water (floor ice and curtain ice) and; (3) condensation of water vapor (hoar ice), all (except floor ice) showed kinetic isotope effects during the freezing of water. This is made evident in the  $d - \delta D$  diagram where the ice formations show no relation because they are scattered across broad horizontal bands.
2. The cryogenic calcite powders, which precipitate during the formation of the seasonal ice formations, also show kinetic isotope effects. Their  $\delta^{13}C$  values are among the highest measured in cold-temperature carbonates and are caused by the rapid rate of freezing, which results in strong C disequilibrium between the water and precipitating calcite, the latter showing an increase in heavy isotopes. The  $\delta^{18}O$  composition of the cryogenic calcite powders also show elevated values associated with kinetic freezing.
3. The cryogenic calcite powders showed varied crystal habits. Rhombs, aggregated rhombs, spheres and needles were all observed under SEM. The rhombs crystal habit was observed at room temperature whereas the spheres and needles were observed at sub-freezing temperatures with cryogenic storage of the samples. This suggests that the sphere structures might represent vaterite, a polymorph of calcite stable only at low temperature. This indicates that not all sphere crystal habits can be attributed to biogenic origin for calcite, as in Caverne de l'Ours, the formation of cryogenic calcite is purely abiotic.

#### ACKNOWLEDGEMENTS

This work was supported by a Canadian Space Agency internal research fund to DL and Natural Sciences and Engineering Research Council of Canada (NSERC) grants to BL and IDC. We would like to thank R. Mineau, W. Abdy and P. Middlestead for their technical assistance in the laboratories. M.S. Field (editor), I. Sasowsky (associate editor), K. Zak, and an anonymous referee provided helpful reviews of the manuscript.

#### REFERENCES

- Albright, J.N., 1971, Vaterite stability: *American Mineralogy*, v. 56, p. 620–624.
- Braissant, O., Cailleau, G., Dupraz, C., and Verrecchia, E.P., 2003, Bacterially induced mineralization of calcium carbonate in terrestrial environments: The role of exopolysaccharides and amino acids: *Journal of Sedimentary Research*, v. 73, p. 485–490.
- Clark, I.D., and Lauriol, B., 1992, Kinetic enrichment of stable isotopes in cryogenic calcite: *Chemical Geology*, v. 102, p. 217–228.
- Clark, I.D., and Lauriol, B., 1997, Aufeis of the Firth River basin, Northern Yukon, Canada: Insights into permafrost hydrogeology and karst: *Arctic and Alpine Research*, v. 29, p. 240–252.
- Courty, M.A., Marlin, C., Dever, L., Tremblay, P., and Vachier, P., 1994, The properties, genesis and environmental significance of calcitic pendants from the high Arctic (Spitsbergen): *Geoderma*, v. 61, p. 71–102.
- Dansgaard, W., 1961, The isotopic composition of natural waters: *Meddelelser om Gronland*, v. 165, p. 1–120.
- Dondale, C.D., Redner, J.H., Paquin, P., and Levi, H.W., 2003, The Insects and Arachnids of Canada: Part 23, The Orb-weaving Spiders of Canada and Alaska. Ottawa, Canada, National Research Council of Canada, 371 p.
- Dresser, J.A., and Denis, T.C., 1946, La géologie de Québec, géologie descriptive: Quebec, Canada, Ministère des Mines, Québec, Rapport géologique 20, 647 p.
- Elver, M.S., 1994, The stratigraphic and isotopic characteristics of an Arctic Icing, Bylot Island, N.W.T. [M.Sc. thesis]: Ottawa, Canada, Carleton University, [http://www.climate.weatheroffice.ec.gc.ca/climate\\_normals/](http://www.climate.weatheroffice.ec.gc.ca/climate_normals/)
- Fairchild, I.J., Bradley, L., and Spiro, B., 1993, Carbonate diagenesis in ice: *Geology*, v. 21, p. 901–904.
- Fairchild, I.J., Killawee, J.A., Spiro, B., and Tison, J.-L., 1996, Calcite precipitates formed by freezing processes: kinetic controls on morphology and geochemistry, in Bottrell, S., ed., *Proceedings of the fourth International Symposium on the Geochemistry of the Earth's Surface*, Ilkley, Yorkshire, Wiley, p. 178–183.
- Folk, R.L., 1993, SEM imaging of bacteria and nanobacteria in carbonate sediments and rocks: *Journal of Sedimentary Petrology*, v. 63, p. 990–999.
- Ford, D.C., and Williams, P., 2007, *Karst hydrogeology and geomorphology*: West Sussex, U.K., Wiley, 576 p.
- Grasby, S.E., 2003, Naturally precipitating vaterite (i-CaCO<sub>3</sub>) spheres: unusual carbonates formed in an extreme environment: *Geochimica et Cosmochimica Acta*, v. 67, p. 1659–1666.
- Hagen-Thorn, A., Callesen, I., Armolaitis, K., and Nihlgård, B., 2004, The impact of six European tree species on the chemistry of mineral topsoil in forest plantations on former agricultural land: *Forest, Ecology and Management*, v. 195, p. 373–384.
- Hall, D.K., 1980, Mineral precipitation in North Slope river icings: *Arctic*, v. 33, p. 343–348.
- Hallet, B., 1976, Deposits formed by subglacial precipitation of CaCO<sub>3</sub>: *Geological Society of America Bulletin*, v. 87, p. 1003–1015.
- Heldmann, J.L., Pollard, W.H., McKay, C.P., Andersen, D.T., and Toon, O.B., 2005, Annual development cycle of an icing deposit and associated perennial spring activity on Axel Heiberg Island, Canadian High Arctic: *Arctic, Antarctic and Alpine Research*, v. 37, p. 127–135.
- IAEA/WMO (International Atomic Energy Agency/World Meteorology Organization), 2004, *Global Network of Isotopes in Precipitation*. The GNIP Database, <http://isohis.iaea.org>
- Jouzel, J., and Souchez, R.A., 1982, Melting—refreezing at the glacier sole and the isotopic composition of the ice: *Journal of Glaciology*, v. 28, p. 35–42.
- Killawee, J.A., Fairchild, I.J., Tison, J.L., Janssens, L., and Lorrain, R., 1998, Segregation of solutes and gases in experimental freezing of dilute solutions: implication for natural glacier systems: *Geochimica et Cosmochimica Acta*, v. 62, p. 3637–3655.
- Kim, S.T., and O'Neil, J.R., 1997, Equilibrium and nonequilibrium oxygen isotope effects in synthetic carbonates: *Geochimica et Cosmochimica Acta*, v. 61, p. 3461–3475.
- Kralj, D., Brecevic, L., and Nielson, A.E., 1990, Vaterite growth and dissolution in aqueous solution: 1. Kinetics of crystal growth: *Journal of Crystal Growth*, v. 104, p. 793–800.
- Kretz, R., 1980, Occurrence, mineral chemistry and metamorphism of Precambrian carbonate rocks in a portion of the Grenville Province: *Journal of Petrology*, v. 21, p. 573–620.
- Kretz, R., 2001, Oxygen and carbon isotopic composition of Grenville marble, and an appraisal of equilibrium in the distribution of isotopes between calcite and associated minerals, Otter Lake, Quebec, Canada: *The Canadian Mineralogist*, v. 39, p. 1455–1472.
- Lacelle, D., 2007, Environmental setting, (micro)morphologies, and stable C-O isotope composition of cold climate carbonate precipitates – a review and evaluation of their potential as paleoclimatic indicators: *Quaternary Science Reviews*, v. 26, p. 1670–1689.
- Lacelle, D., Lauriol, B., and Clark, I.D., 2004, Seasonal isotopic imprint in moonmilk from Caverne de l'Ours: implications for climatic reconstruction: *Canadian Journal of Earth Sciences*, v. 41, p. 1411–1423.



- Lacelle, D., Lauriol, B., and Clark, I.D., 2006, Effect of chemical composition of water on the oxygen-18 and carbon-13 signature preserved in cryogenic carbonates, Arctic Canada: implications in paleoclimatic studies: *Chemical Geology*, v. 234, p. 1–16.
- Majoube, M., 1971, Fractionnement en oxygène-18 et en deutérium entre l'eau et sa vapeur. *Journal of Chemical Physics*, v. 197, p. 1423–1436.
- Marion, G.M., 2001, Carbonate mineral solubility at low temperatures in the Na-K-Mg-Ca-H-Cl-SO<sub>4</sub>-OH-HCO<sub>3</sub>-CO<sub>3</sub>-CO<sub>2</sub>-H<sub>2</sub>O system: *Geochimica et Cosmochimica Acta*, v. 65, p. 1883–1896.
- Marlin, C., Dever, L., Vachier, P., and Courty, M-A., 1993, Variations chimiques et isotopiques de l'eau du sol lors de la reprise en gel d'une couche active sur pergélisol continu (Presqu'île de Brogger, Svalbard): *Canadian Journal of Earth Sciences*, v. 30, p. 806–813.
- Murase, N., Ruike, H., Matsunaya, N., Hagakawa, M., Kaneko, Y., and Ono, Y., 2001, Spider silk has an ice nucleation activity: *Naturwissenschaften*, v. 88, p. 117–118.
- Omelson, C.R., Pollard, W.H., and Marion, G.M., 2001, Seasonal formation of ikaite (CaCO<sub>3</sub> · 6H<sub>2</sub>O) in saline spring discharge at Expedition Fjord, Canadian High Arctic: assessing conditional constraint for natural crystal growth: *Geochimica et Cosmochimica Acta*, v. 65, p. 1429–1437.
- Pauly, H., 1963, Ikaite, a new mineral from Greenland: *Arctic*, v. 16, p. 263–264.
- Prévost, C., and Lauriol, B., 1994, Variabilité de l'érosion actuelle et Holocene: le cas des marbres de Grenville en Outaouais Québécois: *Géographie Physique et Quaternaire*, v. 48, p. 297–303.
- Pollard, W., 1983, A study of seasonal frost mounds, North Fork Pass, northern interior Yukon Territory [Ph.D. thesis]: Ottawa, Canada, University of Ottawa.
- Richter, D.K., and Riechelmann, D.F.C., 2008, Late Pleistocene cryogenic calcite spherulites from the Malachitdom Cave (NE Rhenish Slate Mountains, Germany): origin, unusual internal structure and stable C-O isotope composition: *International Journal of Speleology*, v. 37, p. 119–129.
- Rowe, J.S., 1972, Forest Regions of Canada. Environment of Canada, Canadian Forestry Service, Publication No. 1300, 172 p.
- Silk, S.T., 1970, Factors governing polymorph formation in calcium carbonate [PhD thesis]: New York, New York University.
- Souchez, R.A., and Jouzel, J., 1984, On the isotopic composition in δD and δ<sup>18</sup>O of water and ice during freezing: *Journal of Glaciology*, v. 30, p. 369–372.
- Souchez, R.A., and deGrotte, J.M., 1985, δD- δ<sup>18</sup>O relationships in ice formed by subglacial freezing: paleoclimatic implications: *Journal of Glaciology*, v. 109, p. 599–602.
- Souchez, R.A., Jouzel, J., Lorrain, R., Sleewaegen, S., Stiévenard, M., and Verbeke, V., 2000, A kinetic isotope effect during ice formation by water freezing: *Geophysical Research Letters*, v. 27, p. 1923–1926.
- Suess, E., Balzer, W., Hesse, K.-F., Müller, P.J., Ungerer, C.A., and Wefer, G., 1982, Calcium carbonate hexahydrate from organic-rich sediments of the antarctic shelf: Precursors of glendonites: *Science*, v. 216, p. 1128–1131.
- Turnbull, A.G., 1973, A thermodynamic study of vaterite: *Geochimica et Cosmochimica Acta*, v. 37, p. 1593–1601.
- Vecht, A., and Ireland, T.G., 2000, The role of vaterite and aragonite in the formation of pseudo-biogenic carbonate structures: implications for martian exobiology: *Geochimica et Cosmochimica Acta*, v. 64, p. 2719–2725.
- White, A.F., Bullen, T.D., Vivit, D.V., Schultz, M.S., and Clow, D.W., 1999, The role of disseminated calcite in the chemical weathering of granitoid rocks: *Geochimica et Cosmochimica Acta*, v. 63, p. 1939–1953.
- Zak, K., Urban, J., Cilek, V., and Hercman, H., 2004, Cryogenic cave calcite from several Central European caves: age, carbon and oxygen isotopes and a genetic model: *Chemical Geology*, v. 206, p. 119–136.
- Zak, K., Onac, B.P., and Persoiu, A., 2008, Cryogenic carbonates in cave environments: a review: *Quaternary International*, v. 187, p. 84–96.